

Metal-insulator transition in quasi-two-dimensional Mo-C films

S. J. Lee and J. B. Ketterson

Physics and Astronomy Department and Materials Research Center, Northwestern University, Evanston, Illinois 60208

Nandini Trivedi

Materials Science Division, Argonne National Laboratory, 9700 South Cass Avenue, Argonne, Illinois 60439

(Received 28 October 1991; revised manuscript received 31 July 1992)

We have studied the insulator-to-metal transition in Mo-C films by tuning the thickness from 2.6 to 20 Å. The temperature dependence of the conductivity evolves from hopping transport, for the thin insulating films, to a $\ln T$ dependence for the thicker metallic films. In the insulating regime we find a variable range Mott hopping law at high temperatures crossing over to Efros-Shklovskii hopping at lower temperatures with the opening of a soft Coulomb gap. We also obtain the dependence of the characteristic parameters on the film thickness.

I. INTRODUCTION

The nature of the insulator-metal transition in disordered systems has been a problem of long-standing interest. Theoretically, considerable progress has been made in understanding the behavior of a *single* electron in a random potential. According to the scaling theory of localization,^{1,2} for $d \leq 2$ all states remain localized for arbitrarily small disorder, whereas for $d > 2$ there is a true transition from a localized to a conducting state as the degree of disorder is reduced. It is clear, at least in the insulating state, that the screening is poor and therefore the effects of electron-electron interactions should be very important.³ From the analysis of various experiments these interaction effects are found to be important in the metallic regime as well.^{4,5} While some progress has been made in understanding the *combined* effects of disorder and interaction,^{6,7} a complete scaling theory has not yet emerged.

The insulator-metal transition has been studied in several three-dimensional (3D) systems, e.g., doped semiconductors,^{8,10,9} alloys,¹¹ and granular metals,¹² driven by decreasing disorder or increasing density of electrons or both. In Si:P, for example, the dopants are a source of both the carriers and disorder. If, in addition, one introduces doping by boron (which contributes hole carriers), the density of carriers is given by $n_P - n_B$ but the disorder is related to $n_P + n_B$. In 2D, there have been detailed studies of the transport behavior in films⁴ and inversion layers in metal-oxide-semiconductor field-effect transistor (MOSFET) devices,¹³ primarily in the weak disorder regime. In the weak-localization regime, a film is two-dimensional if the diffusion length L_{Th} is greater than the film thickness d . Since $L_{Th} \sim 100-1000$ Å, depending on the temperature, it is relatively easy to prepare essentially 2D films according to this criterion, which explains why there is so much data in the weak-localization regime. However, in the insulating regime, the criterion for two dimensionality is that the localization length ξ be greater than d . Far into the insulating regime, ξ becomes very small, on the order of 5–10 Å, which puts stringent constraints on d .

In this paper we report systematic studies of the metal-insulator transition in two dimensions in *continuous* Mo-C films. The controlling parameter is the *thickness* of the films. The thinner films are highly disordered and are insulating. As the films are made thicker the degree of disorder decreases and at a thickness d_{cr} the films *crossover* into the metallic regime; a steep crossover can be seen in the temperature-dependent conductivity [equivalent to the length-dependent conductivity at finite temperatures which changes from an exponential (“insulator”) to a logarithmic (“metal”) dependence]. In the insulating regime, we also investigate a second crossover phenomenon from Mott variable range hopping (VRH) to Efros-Shklovskii (ES) VRH as the temperature is lowered and obtain estimates of the Coulomb gap as a function of d . The ability to prepare very thin films (to approximate a 2D system) and the smaller dielectric constant of Mo-C lead to poorer screening and therefore the possibility of a large (detectable) Coulomb gap. This should be contrasted with 3D studies on Si:As (Ref. 9) where such a gap was not observed.

II. EXPERIMENTAL TECHNIQUES

A series of thin films of Mo-C, sandwiched between protective layers of Si-C, were prepared on single-crystal sapphire substrates by the reactive sputtering of Mo in an atmosphere of 7.5×10^{-5} Torr acetylene and 3.0×10^{-3} Torr argon.¹⁴ The Mo-C sandwiched films are electrically continuous down to 2.6 Å. Furthermore, the rather structureless x-ray data indicate that the films are amorphous and not polycrystalline in nature. Also these films are not granular since the $I-V$ characteristics are linear. The thickness of the films was controlled by the deposition rates. After film deposition, Au was sputtered with a mask to provide an Ohmic contact and the standard four-probe method was used to measure the sheet resistance with the current restricted to the linear $I-V$ region. Figure 1 shows the thickness dependence of the films at a fixed temperature, $T=20$ and 300 K. There are several contributions to the resistivity, among them, Anderson localization due to disorder, strong Coulomb interac-

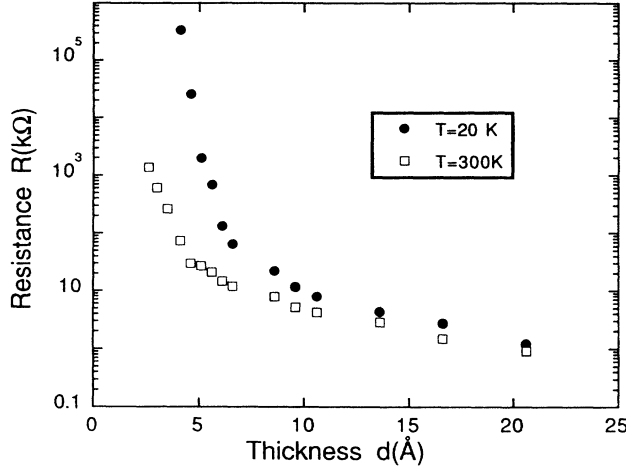


FIG. 1. Thickness dependence of Mo-C films at $T=20$ and 300 K.

tions, surface scattering from a rough surface, and percolation effects from a tenuously connected film, at least in the very thin films.¹⁵ In the analysis presented below we consider the first two contributions, i.e., Coulomb interactions in the presence of bulk disorder. The effect of surface scattering, including the quantum size effects, which are important for the thin films, have been studied previously.¹⁶ However, the combined effects of surface scattering and Coulomb interactions on the resistivity is still an open question.

III. RESULTS AND DISCUSSION

A. Insulating regime (2.6–6.6 Å)

Within a single-particle picture, the crossover from the metallic to insulating state can be viewed as arising from increasing disorder as the films are made thinner. This changes the position of the mobility edge, E_c , which is an energy scale separating the “insulating” and “metallic” regimes. (In 3D, E_c is a definite energy as opposed to an energy scale separating the localized and extended states.) If $E_c > E_F$, the Fermi energy, the film is insulating and in the opposite case, metallic. The films show different types of behavior depending on the temperature. At high temperatures, the electrons hop from a localized state below E_F to the mobility edge. The difference in energy $E_c - E_F$ is provided by phonons and the conductivity is described by an Arrhenius-type activated behavior; i.e., $\sigma = \sigma_0 \exp[-(E_c - E_F)/T]$.

At lower temperatures where the typical phonon energy is much less than $E_c - E_F$, transport occurs by phonon-assisted electron hopping between localized states near the Fermi energy. We now summarize Mott’s arguments concerning this process. Consider two localized states at R_i and R_j with energies E_i and E_j , respectively. The probability to tunnel is proportional to the overlap of the wave functions at the two sites, given by $\exp(-2R/\xi)$, where $R = |R_j - R_i|$ and ξ is the localization length (assumed to be the same at the two sites).

Furthermore, the probability of finding a phonon to provide the energy difference between the localized states is proportional to $\exp(-\Delta E/k_B T)$, where $\Delta E = |E_j - E_i|$. Thus the conductivity, which is related to the total transition probability, is

$$\sigma = \sigma_0 e^{-[(2R/\xi) + (\Delta E/k_B T)]} \quad (1)$$

Now, $g(\Delta E)\pi R^2 \Delta E \sim 1$, where $g(\Delta E)$ is the density of states, and (given a specific form for the density of states) we can use this relation to calculate ΔE in the transition probability and maximize it with respect to R . For a constant density of states $g(\Delta E) = g_0$, we find the most-probable-hopping distance $\bar{R}_M = [\xi/(\pi g_0 T)]^{1/3}$. Inserting this in Eq. (1) we find

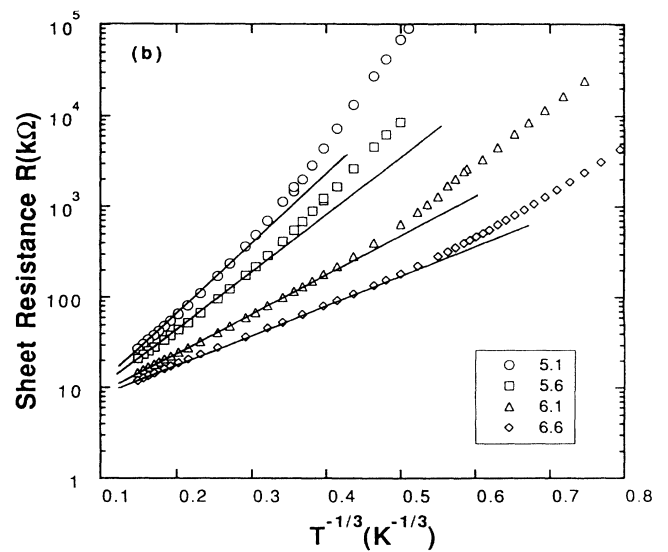
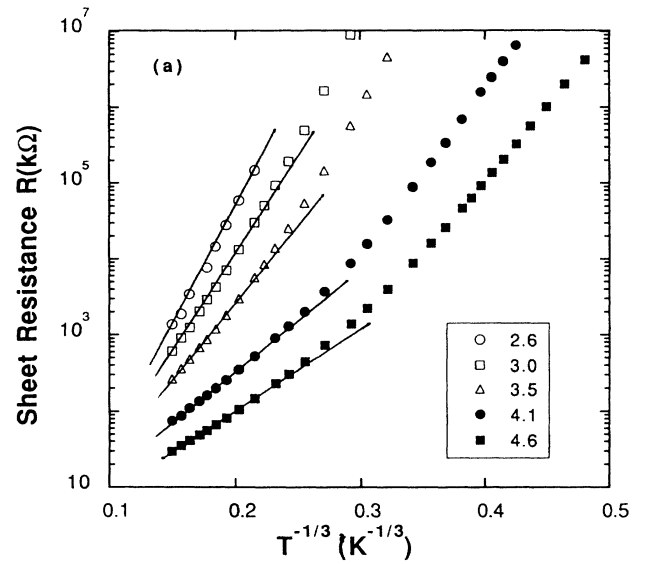


FIG. 2. Sheet resistance in $k\Omega/\square$ vs $T^{-1/3}$ (according to the Mott variable range hopping in 2D) for film thicknesses from 2.6 to 6.6 Å.

TABLE I. Parameters extracted by fitting the high-temperature resistivity to Mott variable range hopping for the thin insulating films.

d (Å)	T_M (K)	ξ (Å)	\bar{R}_M/ξ ($\times T^{-1/3}$)	\bar{R}_M (Å) ($T=10$ K)	$\overline{\Delta E}_M$ (K) ($T=10$ K)
2.6	2.73×10^5	2.95	21.63	29.62	100.40
3.0	1.79×10^5	3.65	18.80	31.86	87.26
3.5	8.20×10^4	5.39	14.48	36.22	67.21
4.1	2.35×10^4	10.07	9.55	44.61	44.31
4.6	1.21×10^4	14.05	7.65	49.88	35.49
5.1	4.43×10^3	23.21	5.47	58.95	25.40
5.6	2.67×10^3	29.89	4.62	63.96	21.46
6.1	9.53×10^2	50.02	3.28	76.03	15.22
6.6	5.70×10^2	64.69	2.76	82.80	12.83

$$\sigma = \sigma_0 \exp[-(T_M/T)^{1/3}], \quad (2)$$

which is the Mott variable range hopping law¹⁷ in 2D characterized by the Mott temperature

$$T_M = 27/(\pi g_0 \xi^2). \quad (3)$$

In terms of T_M , we have the mean hopping distance and the corresponding energy difference given by

$$\bar{R}_M/\xi = \frac{1}{3}(T_M/T)^{1/3} \quad (4)$$

and

$$\overline{\Delta E}_M = \frac{1}{3}T^{2/3}T_M^{1/3}. \quad (5)$$

Figure 2 shows the measured sheet resistance versus $T^{-1/3}$ in accordance with the Mott law [Eq. (2)]. A reasonable fit is obtained only over a very limited range in temperature and the data show deviations at lower temperatures. In Table I, we give the values of various parameters obtained by fitting with the Mott law. We have extracted T_M from the fit and used it to calculate \bar{R}_M/ξ and $\overline{\Delta E}_M$ [from Eqs. (4) and (5), respectively] for films with different thicknesses d . The hopping distance (in

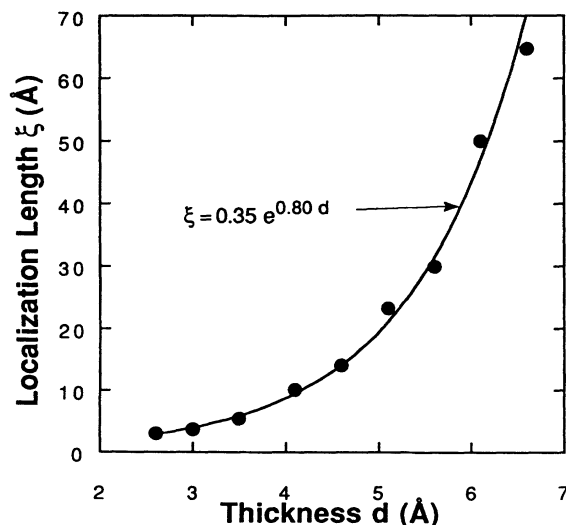


FIG. 3. Localization length ξ vs film thickness d (Å).

units of the localization length) is found to decrease nearly exponentially with increasing thickness. In order to obtain some estimates of the various lengths, we assumed free particle dispersion, which implies a constant density of states in 2D given by $g_0 = m/(\hbar^2 \pi)$. Using this in Eq. (3) we calculate the localization length shown in Fig. 3, which grows exponentially ($\xi \sim \exp[0.8d]$) as the films become more metallic.

As the temperature is lowered further, the effects of correlations between electrons become more important. When the states are localized, their ability to screen the $1/r$ Coulomb interaction between the electrons is considerably reduced. As shown by Efros and Shklovskii¹⁸ (ES), this effect modifies the density of states by opening up a “soft” gap of the form $g(\Delta E) = (2/\pi)|\Delta E - \mu|(\epsilon/e^2)^2$ in two dimensions, where ϵ is the dielectric function. Thus

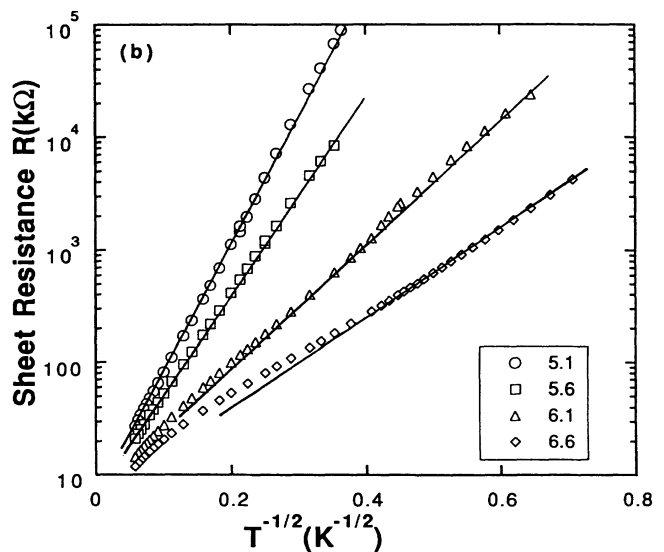
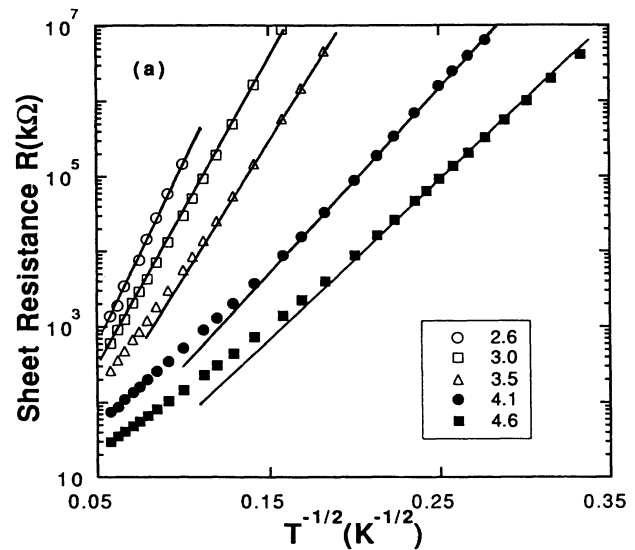


FIG. 4. Sheet resistance in $k\Omega/\square$ vs $T^{-1/2}$ (according to the Efros-Shklovskii variable range hopping that includes electron correlation effects in 2D) for film thicknesses from 2.6 to 6.6 Å.

TABLE II. Parameters extracted by fitting the low-temperature resistivity to Efros-Shklovskii hopping for the thin insulating films.

d (Å)	T_{ES}	\bar{R}_{ES}/ξ ($\times T^{-1/2}$)	\bar{R}_{ES} (Å) ($T=1$ K)	$\overline{\Delta E}_{ES}$ (K) ($T=1$ K)	$\epsilon\xi$ (Å)	ϵ	E_{CG} (K)	T^* (K)
2.6	1.27×10^4	28.21	83.22	56.42	36.70	12.44	159.4	20.01
3.0	9.02×10^3	23.75	86.69	47.50	51.81	14.19	121.8	16.50
3.5	6.04×10^3	19.43	104.73	38.86	77.36	14.35	119.4	23.67
4.1	2.71×10^3	13.01	131.01	26.02	172.51	17.13	83.88	26.04
4.6	1.85×10^3	10.74	150.90	21.48	253.39	18.03	75.66	31.13
5.1	7.01×10^2	6.62	153.65	13.24	666.82	28.73	29.80	12.70
5.6	4.32×10^2	5.20	155.43	10.40	1082.70	36.22	18.75	8.17
6.1	1.61×10^2	3.17	158.56	6.34	2907.40	58.12	7.28	3.31
6.6	7.58×10^1	2.18	141.02	4.36	6168.48	95.35	2.70	0.97

the single-particle density of states, for adding or removing an electron to the ground state (and allowing no relaxation processes), is depleted near the Fermi energy. The prefactor $2/\pi$ was obtained within a mean-field treatment;³ more accurate values may be obtained by computer simulations.¹⁹ Using the above form for the density of states, and maximizing the transition probability (as in the above calculation of the Mott hopping law), we find

$$\sigma = \sigma_0 \exp[-(T_{ES}/T)^{1/2}], \quad (6)$$

where

$$T_{ES} = \beta e^2 / (\epsilon \xi) \quad (7)$$

and $\beta = 4\sqrt{2} \approx 5.66$. In terms of T_{ES} , the mean-hopping distance and energy separation are

$$\bar{R}_{ES}/\xi = 1/4(T_{ES}/T)^{1/2} \quad (8)$$

and

$$\overline{\Delta E}_{ES} = (1/2)T_{ES}^{1/2}T^{1/2}. \quad (9)$$

Figure 4 shows the same set of data fitted to the ES form for the conductivity given in Eq. (6). The ES form is seen to fit the data over a wider temperature range

(with some deviation for the thicker films at high temperatures). Table II lists the values of T_{ES} and other derived quantities. Evaluating $\epsilon\xi$ from Eq. (7) and using the values of ξ from Table I, we obtain the behavior of ϵ shown in Table II. As $d \rightarrow d_{cr}$, with increasing film thickness, the insulator-metal crossover is approached from below and both the localization length $\xi(d)$ and the static dielectric function^{20,8} become very large. As seen from Fig. 5, $\epsilon = \epsilon_0 + 4\pi\chi(d)$, where $\epsilon_0 = 11.6$ is the bulk dielectric constant and $\chi(d) = e^2 g_0 \xi(d) \sim \exp(1.1d)$ which is close to the exponent for $\xi(d)$ shown in Fig. 3.

The energy scale over which the density of states deviates from a constant defines the Coulomb gap given by $E_{CG} = e^4 g_0 / \epsilon$ which is also equal to

$$E_{CG} = (27/\pi\beta^2)(T_{ES}^2/T_M). \quad (10)$$

As seen from Fig. 6, the Coulomb gap is reduced with increasing film thickness because of improved screening in the thicker samples. One expects to see a crossover from Mott hopping to Efros-Shklovskii hopping as the temperature is lowered and the electrons become sensitive to the presence of the Coulomb gap in the density of states. This should occur at a temperature T^* such that

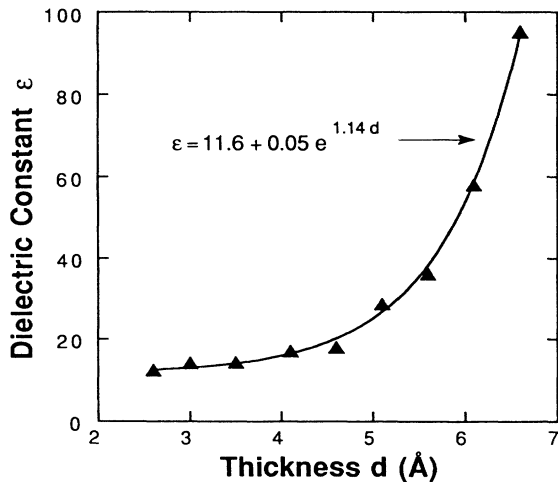


FIG. 5. Dielectric function ϵ vs film thickness d (Å).

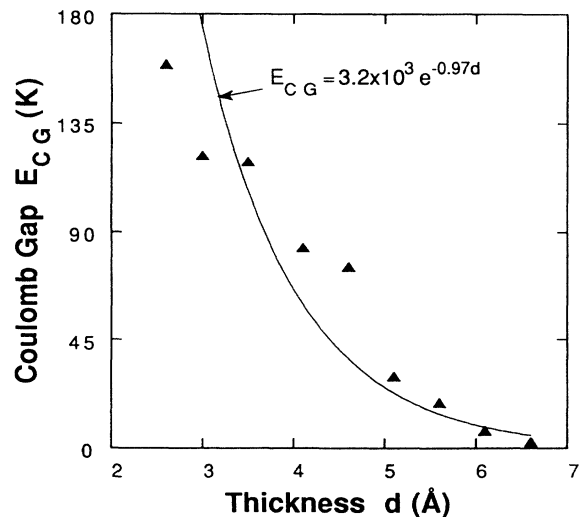


FIG. 6. Coulomb gap E_{CG} (K) vs film thickness d (Å).

$\overline{\Delta E}_M = E_{CG}$, which gives

$$T^* = 3\sqrt{3}(E_{CG}/T_M)^{1/2}E_{CG}. \quad (11)$$

Note that T^* is reduced from E_{CG} by a factor $(E_{CG}/T_M)^{1/2} \approx 10^{-2}$. There is some variation in the value of T^* with film thickness, but the general trend is a decrease in T^* with increasing film thickness; this is consistent with the fact that the Coulomb gap decreases with increasing d . Such a crossover has been seen previously in bulk CdSe.¹⁰

B. Crossover regime

As the insulator-metal crossover is approached, Eq. (7) and the expression for $\chi(d)$ yield $T_{ES} = \sqrt{2}/(\pi g_0 \xi^2)$. The other two temperature scales, T_M from Eq. (3) and E_{CG} from Eq. (10), decrease as $(g_0 \xi^2)^{-1}$. The ratios of these quantities are

$$T_M/T_{ES} = 27/\sqrt{2} \quad (12)$$

and

$$T_{ES}/E_{CG} = \pi 16\sqrt{2}. \quad (13)$$

One expects to see Mott VRH for $\overline{\Delta E}_M(T) > E_{CG}$ when the DOS is smooth. From Eq. (13) this implies $T > 10^{-3}T_M$, which is certainly consistent with our data. To observe ES VRH one requires $\overline{\Delta E}_{ES}(T) < E_{CG}$ in order to be sensitive to the Coulomb gap structure. This implies $T < (27/16\pi)^2 T_{ES}^3/T_M^2 \sim 4 \times 10^{-5}T_M$, which puts a stringent constraint on the temperatures at which ES VRH can be observed since T_M becomes smaller as $d \rightarrow d_{cr}$. In our experiment the maximum resistance that could be measured was $\sim 10^9 \Omega$, so we were unable to record data at temperatures lower than about 1 K. However, even for the 6.6-Å film where $T < 25$ mK, the data are fit rather well by a $\frac{1}{2}$ exponent over an extended temperature regime, implying ES VRH.

Table I also lists \overline{R}_M (and $\overline{\Delta E}_M$) at a fixed temperature (say 10 K); for films with thickness between 2.6 and 6.6 Å, \overline{R}_M increases and is always greater than the localization length ξ (which is also an increasing function of d). However, since we expect $\xi(d)$ to become large near d_{cr} , there appears to be a regime (that we have not yet attained with our films) where in fact $\overline{R}_M < \xi(d)$. In this case one no longer expects the VRH models to be appropriate. An analysis²¹ of this regime has shown that the primary effect is to change the weak temperature dependence of the prefactor in Eq. (2).

C. Metallic regime (8.6–20.6 Å)

Between 8.6 and 20.6 Å we observe a logarithmic dependence¹⁵ of the conductivity for temperatures from 20 to 300 K. Figure 7 shows the data for six films with thicknesses straddling the crossover region. According to weak-localization theory,^{1,2} the Boltzmann conductivity is reduced logarithmically in two dimensions, because of quantum interference of an electron in the random potential of the disordered film. At finite temperatures, the quantum coherence is destroyed over a length scale

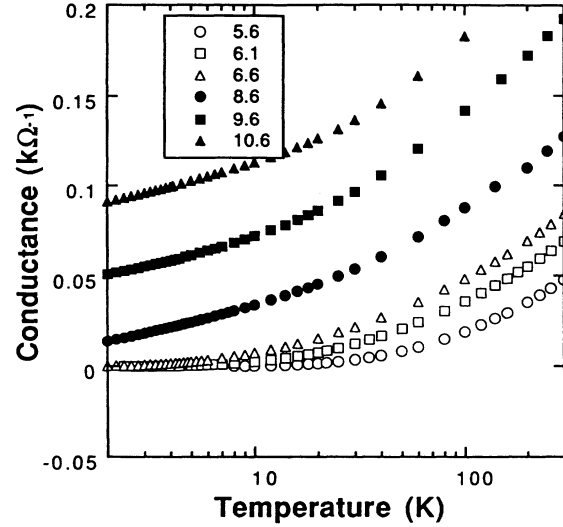


FIG. 7. Temperature dependence of the sheet conductance for Mo-C sandwiches within the crossover region with $d = 6.1, 6.6, 8.6,$ and 9.6 Å.

$L_{Th} = (D\tau_d)^{1/2}$, which is the distance an electron can diffuse in an inelastic (or dephasing) time $\tau_d \gg \tau$ and $D = v_F^2\tau/2$ is the diffusion constant. It is also necessary to include the effects of electron-electron interactions. Since the electron motion is diffusive in the presence of impurities, they spend a longer time in a given region in space compared to the plane-wave states; this leads to an enhanced interaction between electrons. The resulting diffusion pole in the propagators leads to singular behavior in the density of states,⁵ which, in two dimensions, is given by

$$\frac{\delta g(\epsilon)}{g_0} \propto \ln(T\tau). \quad (14)$$

The total correction to the conductivity (from both weak localization and interaction effects²) is

$$\sigma(T) = \sigma_0 + \frac{t\alpha p}{2} \frac{e^2}{\hbar\pi^2} \ln\left[\frac{T}{T_0}\right] + (1-F) \frac{e^2}{\hbar\pi^2} \ln\left[\frac{T}{T_0}\right]; \quad (15)$$

here t is an “antilocalization” factor arising from spin-orbit scattering, α is the number of degenerate valleys, and F is a screening factor. Furthermore, we have assumed that $\tau_d \sim T^{-p}$, where p depends on the specific scattering mechanism. The analysis of the magnetoresistance data suggests the presence of strong spin-orbit scattering in our films.¹⁵ All the samples in the “metallic” regime show a change in slope near 30 K. By fitting our data²² to Eq. (15), we find that over the entire temperature range $F = 0$ (implying strong interaction effects), $\alpha = 3$, and $p \approx 1-2$. For $T < 30$ K, $t \approx 0$, implying that weak-localization effects are cancelled by spin-orbit antilocalization, whereas for $T > 30$ K, $t \approx 1$, showing a small spin-orbit scattering.

These Mo-C films have also shown an interesting insulator-superconductor transition as a function of film

thickness up to 200 Å.²³ Similar behavior has been seen in other ultrathin granular and continuous metallic films.²⁴

IV. CONCLUSION

We have investigated the insulator-metal transition in ultrathin Mo-C films driven by increasing film thickness. The highly 2D nature and small dielectric function of the Mo-C films allows us to probe the insulator-metal crossover. In particular, we have tracked the effects of a Coulomb gap in the density of states as a function of film thickness by studying the temperature dependence of the hopping conductivity. As the crossover region is approached, both the localization length and dielectric function grow exponentially. Thicker films show a logarithmic dependence of the conductivity on temperature, consistent with weak localization and interaction effects in 2D. From a detailed analysis of the dephasing mecha-

nism, we find that spin-orbit scattering becomes important for $T < 30$ K. A detailed theory in the transition region does not exist at the present time. It would be interesting to observe the Coulomb gap directly in the Mo-C system since it is quite large (≈ 10 – 15 meV for the thinnest films) by a spectroscopic method (e.g., photoemission, infrared transmission, or tunneling microscopy).

ACKNOWLEDGMENTS

The research at Northwestern University was supported by the NSF Materials Research Center, the National Science Foundation, and the Office of Naval Research under Grants No. DMR-85-20280, No. DMR-89-07396, and No. N0014-88-K0160, respectively. Work at Argonne National Laboratory was supported by the U.S. Department of Energy under Grant No. W-31-109-ENG-38.

¹E. Abrahams, P. W. Anderson, D. C. Licciardello, and T. V. Ramakrishnan, *Phys. Rev. Lett.* **42**, 673 (1979).

²P. A. Lee and T. V. Ramakrishnan, *Rev. Mod. Phys.* **57**, 287 (1985).

³A. L. Efros and B. I. Shklovskii, *J. Phys. C* **8**, L49 (1975); A. L. Efros, *ibid.* **9**, 2021 (1976).

⁴G. Bergman, *Phys. Rep.* **107**, 1 (1984).

⁵B. L. Altschuler and A. G. Aronov, *Solid State Commun.* **30**, 115 (1979); B. L. Altschuler, A. G. Aronov, and P. A. Lee, *Phys. Rev. Lett.* **44**, 1288 (1980).

⁶W. L. McMillan, *Phys. Rev. B* **24**, 2739 (1981).

⁷D. Belitz and T. R. Kirkpatrick, *Phys. Rev. Lett.* **63**, 1296 (1989); M. Milovanovic, S. Sachdev, and R. N. Bhatt, *ibid.* **63**, 82 (1989).

⁸T. F. Rosenbaum, R. F. Milligan, M. A. Paalanen, G. A. Thomas, R. N. Bhatt, and W. Lin, *Phys. Rev. B* **27**, 7509 (1983).

⁹W. N. Shafarman, D. W. Koon, and T. G. Castner, *Phys. Rev. B* **40**, 1216 (1989).

¹⁰Y. Zhang, P. Dai, M. Levy, and M. P. Sarachik, *Phys. Rev. Lett.* **64**, 2687 (1990).

¹¹W. L. McMillan and J. M. Mochel, *Phys. Rev. Lett.* **46**, 556 (1981); B. W. Dodson, W. L. McMillan, J. M. Mochel, and R. Dynes, *ibid.* **46**, 45 (1981); G. Hertel, D. J. Bishop, E. G. Spencer, J. M. Rowell, and R. C. Dynes, *ibid.* **50**, 743 (1983).

¹²R. C. Dynes and J. P. Garno, *Phys. Rev. Lett.* **46**, 137 (1981).

¹³R. G. Wheeler, K. K. Choi, A. Goel, R. Wisnieff, and D. E. Prober, *Phys. Rev. Lett.* **49**, 1674 (1982); Y. Kawaguchi and S. Kawaji, *J. Phys. Soc. Jpn.* **48**, 699 (1980).

¹⁴H. Q. Yang, B. Y. Jin, Y. H. Shen, H. K. Wong, J. E. Hilliard, and J. B. Ketterson, *Rev. Sci. Instrum.* **56**, 607 (1985).

¹⁵S. J. Lee and J. B. Ketterson (unpublished).

¹⁶N. Trivedi and N. W. Ashcroft, *Phys. Rev. B* **38**, 12 298 (1988).

¹⁷N. F. Mott, *Metal-Insulator Transitions* (Taylor and Francis, London, 1974).

¹⁸A. L. Efros and B. I. Shklovskii, in *Coulomb Interaction in Disordered Systems with Localized Electronic States*, edited by A. L. Efros and M. Pollak (North-Holland, New York, 1985).

¹⁹S. D. Baranovskii, A. L. Efros, B. L. Gelmont, and B. I. Shklovskii, *J. Phys. C* **12**, 1023 (1979).

²⁰H. F. Hess, K. DeConde, T. F. Rosenbaum, and G. A. Thomas, *Phys. Rev. B* **25**, 5578 (1982).

²¹A. Miller and E. Abrahams, *Phys. Rev. B* **120**, 745 (1960).

²²S. Hikami, A. Larkin, and Y. Nagaoka, *Prog. Theor. Phys.* **63**, 707 (1980).

²³S. J. Lee and J. B. Ketterson, *Phys. Rev. Lett.* **64**, 3078 (1990).

²⁴H. M. Jaeger, D. B. Haviland, B. G. Orr, and A. M. Goldman, *Phys. Rev. B* **40**, 182 (1989); D. B. Haviland, Y. Liu, and A. M. Goldman, *Phys. Rev. Lett.* **62**, 2180 (1989).